Pergamon

Int. J. Heat Mass Transfer. Vol. 40, No. 1, pp. 49–59, 1997

0017–9310/97 $15.00 + 0.00

PII: S0017-9310(96)00073-7

Regions of validity of the geometric optics approximation for angular scattering from very rough surfaces

KAKUEN TANG, RALPH A. DIMENNA and RICHARD O. BUCKIUS†

Department of Mechanical and Industrial Engineering, University of Illinois, 1206 West Green Street, Urbana, IL 61801, U.S.A.

(*Received* 20 *July* 1995 *and in revised form* 13 *February* 1996)

Abstract—The geometric optics approximation for radiative scattering from rough surfaces is compared with exact scattering predictions from electromagnetic theory. Rigorous electromagnetic scattering theory is numerically formulated based on the extinction theorem. Radiative predictions from one-dimensional random rough surface profiles are calculated for a broad range of surface length scales (correlation lengths, rms roughnesses), wavelengths and incident angles. A directional criterion is used to compare the exact and the approximate results based on very small angular regions. Surface parameter domains for the regions of accuracy of the geometric optics approximation are quantified and presented as a function of surface slope and roughness. Copyright © 1996 Elsevier Science Ltd.

INTRODUCTION

The geometric optics approximation is a ray tracing or energy approximation and is probably the most common approach used in thermal radiation calculations. This approximation is used in many instances to quantify the thermal radiative properties, such as reflection, transmission, absorption, and emission, and to characterize the directional selectivity of surfaces [1–3]. While geometric optics has been previously used to determine the properties of surfaces, the regions of validity of the approximation compared with electromagnetic theory have not been quantified. This work quantifies the regions of validity for the geometric optics approximation on a directional basis by comparison with rigorous electromagnetic theory predictions.

Radiative scattering from rough surfaces can be predicted by a number of approximations and exact solutions. The electromagnetic scattering theory is the exact approach based on the extinction theorem [4] used to quantify the directional nature of surface scattering [5–9]. The Fresnel and Kirchhoff approximations are common specular approximations to electromagnetic scattering and have been extensively compared with exact solutions [10–14]. Thorsos [11] presents results which show agreement between the Kirchhoff approximation and geometric optics for moderate ratios of the correlation length to the incident wavelength from 2.0 to 4.75, and Thorsos limits his ratios of the deviation to the incident wavelength from 0.045 to 0.701. Since Thorsos' work is concerned with specular approximations, very rough surfaces are not examined. Also, only a limited range of incident angles are examined. The geometric optics approximation to electromagnetic scattering theory is both a specular and diffuse approximation. Since the geometric optics approximation includes multiple scattering into the solution, it can accurately characterize diffuse behavior when the rms deviation becomes very rough. However, the geometric optics approximation comparisons with electromagnetic theory have not been quantified.

The geometric optics approximation ray traces the energy incident on a rough surface until it leaves the surface, thereby including multiple scatters from various surface elements. Each surface interaction is modeled as a reflection from a locally optically smooth surface (Fresnel approximation). Therefore, in the limit of a plane surface, the geometric optics approximation reduces to the Fresnel approximation since only a single scatter from the surface occurs. As shown in this effort, the geometric optics approximation predicts forward, diffuse and retro-reflection. Even though the geometric optics approximation is a multiple scattering solution, it does not accurately incorporate all surface scattering phenomena.

Since the geometric optics approximation is computationally less expensive than the exact solution, the geometric parameter domain for accurate predictions by this approximation is important to its usefulness. This work establishes a rather restrictive directional criterion for agreement between the geometric optics approximation and electromagnetic theory and presents the parameter domain of validity of the geometric optics approximation.

† Author to whom correspondence should be addressed.

NOMENCLATURE

E	error between exact and approximate solutions
$\boldsymbol{E}$	electric field intensity vector
F	electric field intensity derivative
G	Green's function
$\boldsymbol{H}$	magnetic field intensity vector
$H_o^{(1)}$	Hankel function of first kind of order 0
I	intensity
i	unit imaginary number
$\hat{\mathbf{i}}, \hat{\mathbf{j}}, \hat{\mathbf{k}}$	unit vectors
k	wavevector component
L_x	surface length
$\hat{\mathbf{n}}$	surface outward normal vector
N	number of surface points
r	scattering reflection function
$\mathbf{r}, \mathbf{R}$	position vectors
S	surface perimeter
x, y, z, x', z'	surface coordinates.

Greek symbols

δ	Dirac delta function
Φ	radiant power flow
λ	wavelength
θ	angle of energy
ρ'', ρ'	bi-directional reflection function, directional reflectivity
σ	standard deviation
τ	surface correlation length
Ω	solid angle
ζ	surface profile.

Subscripts

a	approximate solution
cr	critical value
d	directional criterion
e	exact solution
o	incident
s	scattered
SR	specular reflection
TE	transverse electric polarization
TM	transverse magnetic polarization
x, y, z	coordinates.

Superscripts

$''$	bi-directional
$>$	above.

ROUGH SURFACE SCATTERING SOLUTIONS

Bi-directional reflection function

The bi-directional reflection function, the radiative property of interest for angular scattering comparisons, is expressed in terms of the incident power and the scattered power. From the Poynting theorem relation [15], the bi-directional reflection function is expressed as π times the ratio of the reflected radiant power per unit solid angle per unit projected area to the incident radiant power [16]. This function is

$$\rho''_\lambda(\theta_o, \theta_s) = \frac{\dfrac{\pi \dfrac{d\Phi_s}{d\Omega_s}}{\cos\theta_s}}{\dfrac{d\Phi_o}{d\Omega_o}} \quad (1)$$

where Φ is the radiant power, Ω is the solid angle, and the subscripts o and s denote incident and scattered, respectively. Integrating equation (1) over all the scattering angles for a given incident angle yields the hemispherical reflection. The following sections formulate the exact method for obtaining Φ_s and Φ_o for use in equation (1).

Random rough surfaces

A surface described by $\zeta(x)$ as shown in Figs. 1(a) and (b) separates a vacuum region ($z > \zeta(x)$) from a perfectly conducting material. The surface is one-dimensional, only varying in the x direction, so that scattering is considered in the plane of incidence. The random rough surfaces are described by a stationary, Gaussian process [6, 8, 17] with zero mean deviation from $z = 0$,

$$\langle \zeta(x) \rangle = 0 \quad (2)$$

and a correlation length, τ, defined by the width of a Gaussian correlation function over which the correlation diminishes by a factor of e, as

$$\langle \zeta(x)\zeta(x') \rangle = \sigma^2 \exp[-(x-x')^2/\tau^2]. \quad (3)$$

Figure 1(a) shows multiple realizations of a surface with a correlation length to wavelength ratio, τ/λ, of 2.0 and a rms deviation to wavelength ratio, σ/λ, of 0.20, corresponding to a slope of $\sigma/\tau = 0.1$. The horizontal axis is x/λ and the vertical axis is the surface profile to wavelength, $\zeta(x/\lambda)/\lambda$. The incident and scattering angles are defined by the angular scattering representation shown in the inset of Fig. 1(a). Figure 1(b) shows the surface realizations of a surface with parameters $\tau/\lambda = 1.0$, $\sigma/\lambda = 3.0$ and $\sigma/\tau = 3.0$. These two figures demonstrate the difference between surfaces that exhibit specular scattering behavior [Fig. 1(a)] and surfaces that are diffuse scatterers [Fig. 1(b)].

Electromagnetic theory

Electromagnetic theory provides rigorous solutions for the scattering of incident waves from interfaces. A

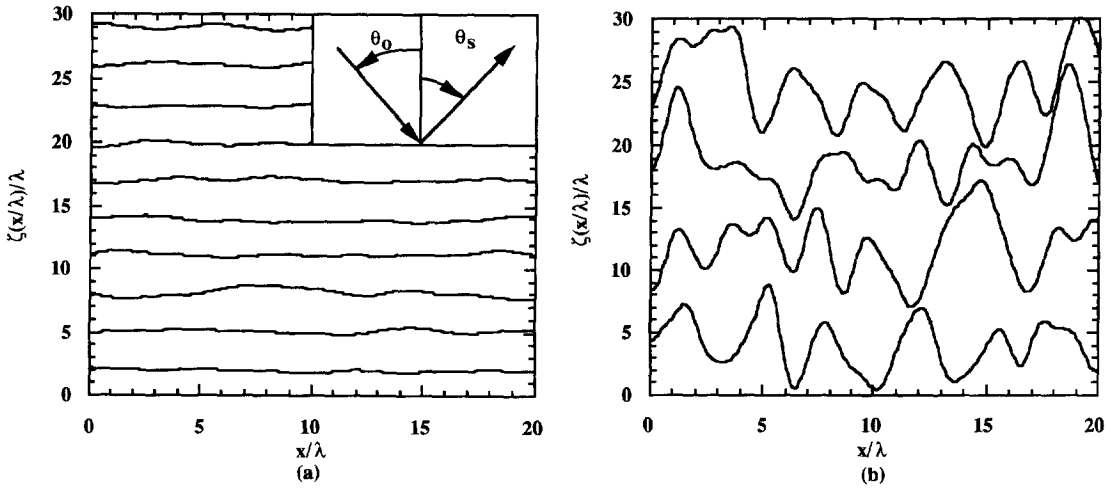

Fig. 1. Multiple realizations of surfaces: (a) $\sigma/\tau = 0.1$, $\sigma/\lambda = 0.2$, $\tau/\lambda = 2.0$ and (b) $\sigma/\tau = 3.0$, $\sigma/\lambda = 3.0$, $\tau/\lambda = 1.0$.

linearly polarized, monochromatic, plane electromagnetic incident wave strikes the surface at an incident angle, θ_o, as depicted in Fig. 1(a). Since only the plane of incidence is of interest, there is no depolarization for either the transverse magnetic (TM) or transverse electric (TE) incident wave. Therefore, the electric field vector for TE polarization and the magnetic field vector for TM polarization have only components perpendicular to the plane of incidence.

The reflected field is obtained by solving the Helmholtz equation above the surface. The Helmholtz equation describing the magnetic and electric fields [15] is used to describe the fields above the surfaces typified by Figs. 1(a) and (b). Both the magnetic field, $\boldsymbol{H}$, and the electric field, $\boldsymbol{E}$, satisfy a continuity condition on the component tangent to the surface [15]. H_y is the only component of $\boldsymbol{H}$ which remains for TM polarization and E_y is the only component of $\boldsymbol{E}$ which remains for TE polarization. By using Maxwell's equations [15], the jump conditions for the electric and magnetic fields are obtained [9, 18].

The Helmholtz equation in two dimensions, with a line source is

$$\nabla^2 G_o + k_o^2 G_o = -4\pi\delta(x-x_o)\delta(z-z_o) \qquad (4)$$

where G_o is the two-dimensional Green's function. After a coordinate transformation, the two-dimensional Green's function is expressed in terms of the zeroth order Hankel function of the first kind [19] as

$$G_o(|\mathbf{r}-\mathbf{R}|) = i\pi H_o^{(1)}(k_o|\mathbf{r}-\mathbf{R}|). \qquad (5)$$

The new coordinates are given by $\mathbf{r} = x\hat{\mathbf{i}} + z\hat{\mathbf{k}}$ and $\mathbf{R} = x'\hat{\mathbf{i}} + z'\hat{\mathbf{k}}$.

In order to obtain the scattered power in terms of the scattering angle, θ_s, equation (5) is integrated over the volumetric vacuum above the surface. By use of Green's theorem, the volumetric integral of equation (4) is expressed as an integral over an arbitrary surface, S. After substituting the Helmholtz equation [15] and equation (5), the volumetric integral is reduced, and the surface integral for TM polarization is expressed as

$$-4\pi H_y^{>}(x,z) = \int_S \left[H_y^{>}(x',z') \frac{\partial G_o(x,z;x',z')}{\partial n} - G_o(x,z;x',z') \frac{\partial H_y^{>}}{\partial n} \right] da' \qquad (6)$$

where the superscript $>$ denotes the magnetic field above the surface. For TE polarization, the surface integral is the same as equation (6) with E_y replacing H_y. Equation (6) is an integral over an arbitrary surface, S, and da' is an arbitrary differential. Since the surface is arbitrary, the integral is taken over a surface at infinity added to an integral taken over the material surface. The integral over the surface at infinity is interpreted as the incident field [4]. In this way, equation (6) becomes

$$-4\pi H_y^{>}(x,z) = -4\pi H_y^{>}(x,z)_o + \int_{S_\zeta} \left[H_y^{>}(x',z') \frac{\partial G_o(x,z;x',z')}{\partial n} - G_o(x,z;x',z') \frac{\partial H_y^{>}(x',z')}{\partial n} \right] da'. \qquad (7)$$

Again, the formulation for the TE polarization is the same with E_y replacing H_y. By substituting the jump conditions and the definition of the normal derivative [10, 18] into equation (6) and the analogous equation for TE polarization, the integral equations for the magnetic and electric fields are

$$H_y^{>}(x,z) = H_y^{>}(x)_o + \frac{1}{4\pi}\int_{-\infty}^{\infty} \left[H(x') \left(-\zeta'(x') \frac{\partial}{\partial x'} + \frac{\partial}{\partial z'} \right) G_o(x,z;x',z')|_{z'=\zeta(x')} \right] dx' \qquad (8a)$$

$$E_y^{>}(x)_o = \frac{1}{4\pi}\int_{-\infty}^{\infty}\left[G_o(x,z;x',z')F(x')|_{z'=\zeta(x')}\right]dx' \quad (8b)$$

where G_o is given by equation (5) and F is the derivative of the electric field intensity. The Hankel function in G_o has a singularity and must be directly integrated by numerical computation [7, 9]. Equations (8) are the integral equations governing surface scattering from a perfectly conducting surface. With the integral representation of G_o, equations (8) provide the angular scattered fields. The total power scattered into the region above the material surface is calculated from the Poynting power theorem [15]. After evaluating the integral of the power theorem, the power scattered into any angle is found [9, 10, 18]. The scattered power is substituted into equation (1) with the incident power to give the desired result for bi-directional reflection as

$$\rho''_{\lambda TM}(\theta_o,\theta_s) = \frac{1}{8\pi}\frac{1}{L_x\cos\theta_s\cos\theta_o}|r_{TM}(\theta_s)|^2 \quad (9a)$$

$$\rho''_{\lambda TE}(\theta_o,\theta_s) = \frac{1}{8\pi}\frac{1}{L_x\cos\theta_s\cos\theta_o}|r_{TE}(\theta_s)|^2 \quad (9b)$$

where L_x is the length of the surface in the x direction and the scattering reflection functions, $r_{TM}(\theta_s)$ and $r_{TE}(\theta_s)$, are given by

$$r_{TM}(\theta_s) = \int_{-\infty}^{\infty}\{\exp\zeta - ik_o(x\sin\theta_s + \zeta(x)\cos\theta_s)\} \times (ik_o(\zeta'(x)\sin\theta_s - \cos\theta_s)H(x))\}\,dx \quad (10a)$$

$$r_{TE}(\theta_s) = \int_{-\infty}^{\infty} -F(x)\exp\{-ik_o(x\sin\theta_s + \zeta(x)\cos\theta_s)\}\,dx. \quad (10b)$$

The unknowns, $H(x)$ and $F(x)$ in equations (10) represent the magnetic field and the electric field derivative, respectively. For unpolarized radiation, a simple average of equations (10) is taken. The equations for bi-directional reflection can be integrated over the surface to obtain hemispherical reflection, which in the case of perfectly conducting surfaces, must equal unity.

Geometric optics approximation

The geometric optics or ray tracing approximation to the electromagnetic theory predictions of surface scattering is a multiple scattering solution which traces energy from incidence until it leaves the surface. Each scattering is treated as a Fresnel reflection at the local point of interaction. In the limit of a plane surface, the geometric optics approximation becomes the Fresnel or specular approximation. The steps used to calculate the bi-directional reflection function in the geometric optics approximation for general surfaces are as follows:

The rough random surface profiles are generated along with the surface derivatives, tangents and slopes for each surface node. Depending on the roughness, deviation and correlation length of the surface, between 2000 and 2450 surface nodes are used to generate a surface.

The angle of incident energy and the first reflection point are chosen (Fig. 2). The first reflection points are not necessarily the nodes, so there can be more reflection points than nodes. In each surface, at least 20,000 first reflection points are used in the calculations. The reflection points can be either chosen randomly over the entire surface, or they can be equally spaced points in the x dimension [16]. Using equally spaced points in the x dimension gives the same results and takes less computational time.

Using the tangent angle of the reflection point, it is determined whether or not the incident energy strikes the point. If the energy is incident at an angle larger than the tangent angle of the point, it does not strike the point, and then another first reflection point is selected.

The effect of shadowing by the surface is also considered. This effect is most important at large incident angles. Using the ratio of the differential change in the first reflection point and any surface nodes at smaller x (only portions of the surface at smaller x can shadow for the coordinate system of the indicated θ_o), it is determined whether the reflection point is possible. If the energy is incident at an angle larger than any ratio of the differential change, another first reflection point is selected. If the incident energy strikes the point, the reflection angle is found with the surface normal using Snell's Law [16]. Once the energy of this incident ray is calculated by dividing the cosine of the sum of the tangent angle and the incidence angle by the cosine of the tangent angle and the number of first reflection points and multiplying by the surface length then the amount of the reflected energy is determined through the multiplication of the energy of incident ray and the Fresnel coefficient [16]. The coefficient is unity for perfectly conducting surfaces and the amount of reflected energy is equal to that of the incident beam.

To determine the second reflection point, the tangent of the reflection angle is compared with the ratio of the differential change in the point and the nodes along the surface. If the highest node on the surface is examined and the energy does not strike between the first reflection point and this highest node, then the reflected energy is considered scattered energy from the surface. When the reflected energy travels across the ends of the surface without striking the surface, the surface nodes are mirrored on the opposite sides with the surface normals reversed. This ensures that the reflected energy will strike a node on the mirrored surface and be reflected back into the region of interest. By analysing the tangent of the reflection angle in relation with the change in the surface nodes, the second reflection point is determined,

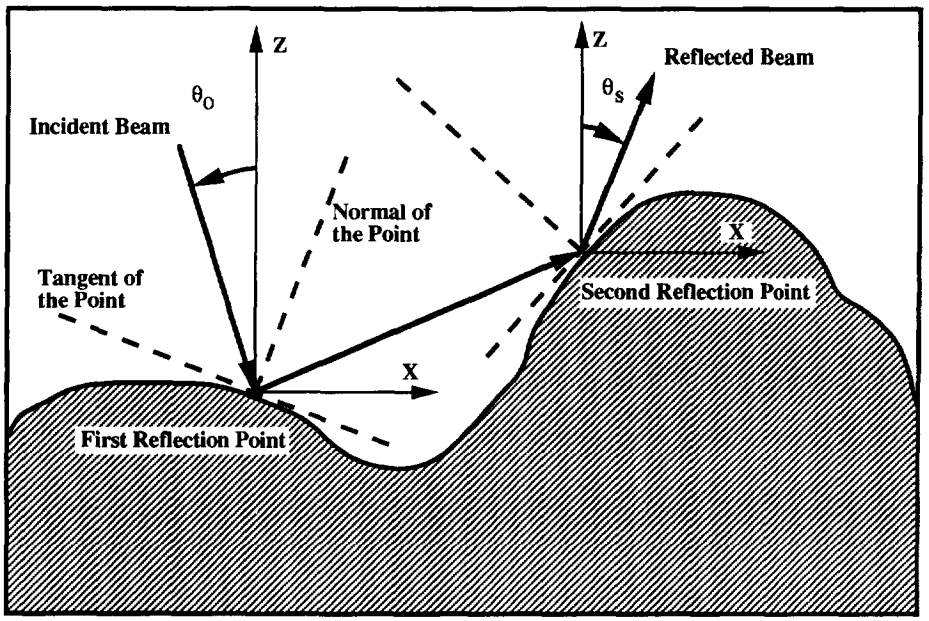

Fig. 2. Rough surface scattering geometry.

and the reflected angle is transformed into the new incident angle. The entire scattering process for successive reflection points and the reflected angles is continued until the reflected energy completely leaves the surface.

When all of the energy has been scattered for all first reflection points at an incident angle, the scattered energy at each scattered angle is divided by the total energy incident on the surface at that incident angle. This result is the differential reflection coefficient from the surface. Once all of the incident angles have been analysed, additional surface profiles are examined until the reflection from approximately 60 surface profiles with the same parameters have been determined. The resulting differential reflection coefficients are then averaged. This ensures a statistically accurate solution. Finally, the bi-directional reflection function is found through dividing the differential reflection coefficient by the cosine of the scattering angle and the size of the angular scattering regions, $\Delta\theta_s$, and multiplying by π.

The bi-directional reflection function is compared with the unpolarized result from equations (9) from the electromagnetic theory. When the energy is incident at an angle larger than the tangent angle of the first reflection point, or the point lies in the shadow, the point doesn't participate in the calculation. For this reason, the number of first reflection points must be sufficient to eliminate any statistical variations in the amount of incident energy striking the surface.

In short, for perfectly conducting surfaces, the approximation is a calculation of the reflection direction equal to the incident direction at a surface point, since all of the energy is reflected. For dielectric surfaces, the Fresnel coefficient is introduced to account for the transmission and reflection by the interface.

Numerical implementation

The scattering equations given by the electromagnetic theory formulation [5–10, 18] are solved by a quadrature scheme. The integral equations are discretized over N intervals of interest over the surface length, L_x, so that the integral equations [i.e. equations (8a) and (8b)], have a matrix form [7–9, 18]. The matrix elements are provided by Maradudin *et al.* [7, 18].

Each of the following bi-directional reflection function results is averaged over approximately 60 rough surface profiles. In general, after 20 surface profiles, the influence of the number of surface profiles on the directional reflected energy is less than 2.0% for both the exact solution and the geometric optics approximation. Each surface length, L_x, is discretized into at most 2450 points in x, depending on the roughness of the surface. Surfaces that are more optically smooth do not require as many points as surfaces which have large values of σ/λ. Similarly, even for very rough cases such as $\sigma/\tau = 3.0$, the influence of surface points on the directional reflected energy is less than 2.0% for more than 2000 points. Surface lengths are typically 100λ–200λ depending on τ/λ. The surface length is made as long as possible to minimize the edge effects from the incident plane wave on the surface. For perfectly conducting surfaces, all of the incident energy must be reflected. Therefore, the hemispherical reflection function for the surface must equal unity. For a dielectric surface, the sum of the hemispherical reflection function and transmission function must be unity. All results presented conserve energy to within 1.0%.

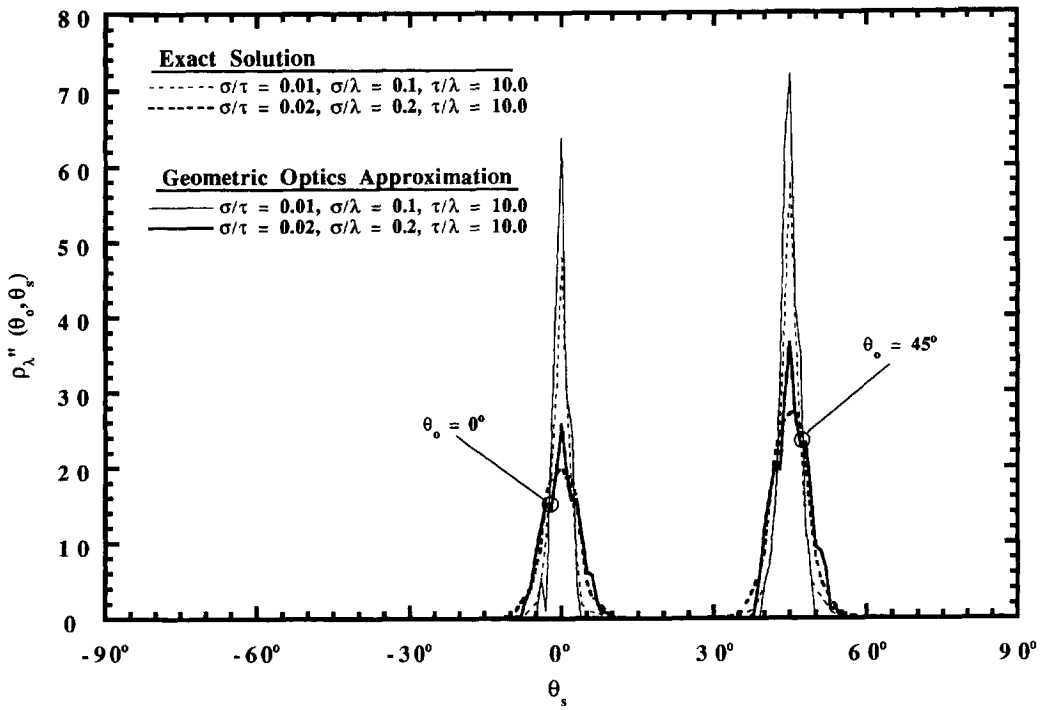

Fig. 3. Comparison of exact solutions with geometric optics approximations for the bi-directional reflection function at $\theta_o = 0°$ and 45° for specular surfaces.

The equations are programmed on a Cray Y-MP4/464 using LAPACK-b1 routines to solve for the unknowns, $H(x)$ and $F(x)$. The specific routines used are CGETRF and CGETRS, which factor the matrix into its LU decomposition and solve the matrix, respectively. The averages $\langle|r_{TM}(\theta_s)|^2\rangle$ and $\langle|r_{TE}(\theta_s)|^2\rangle$ are then used in the bi-directional reflection function given in equations (9). Therefore, the scattering properties of a generic rough surface with given roughness and correlation parameters are determined.

RESULTS

General reflection characteristics

Figures 3–5 present bi-directional reflection results for the geometric optics approximation and electromagnetic theory predictions at incident angles, $\theta_o = 0°$ and 45°. The bi-directional reflection function is presented for scattering angles, θ_s, between $-90°$ and 90°.

The reflection distribution results can be classified into four general categories according to the surface slope [20] defined as σ/τ. For optically smooth surfaces with $\sigma/\tau \ll 1$, the bi-directional reflection function is a specular spike at the scattering angle which mirrors the incident angle. For surfaces that are close to optically smooth, the geometric optics approximation predicts a reflection distribution that is relatively specular and surrounds the scattering angle, $\theta_s = \theta_o$. For surfaces with a larger slope, the geometric optics approximation predicts a more diffuse distribution which deviates significantly from the specular spike. For very rough surfaces with $\sigma/\tau \geqslant 1$, the distribution exhibits strong retro-reflection and a peak occurs at the anti-scattering angle, $\theta_s = -\theta_o$.

Figures 3–5 demonstrate the change in the bi-directional reflection distribution from specular reflection to retro-reflection. The cases in Fig. 3, where the surfaces are described by the slope $\sigma/\tau = 0.01$ and $\sigma/\tau = 0.02$, exhibit specular reflection. In both the exact solution and the geometric optics approximation, high values of reflection for a very small angular region are predicted at the scattering angle, $\theta_s = \theta_o$.

Figure 4 presents the results of two surfaces with intermediate roughness. The surface with $\sigma/\tau = 0.1$ is an example of the case in which the reflection distribution is close to optically smooth. The exact and geometric optics results are a Gaussian-shaped curve about the scattering angle, $\theta_s = \theta_o$. The reflection distribution spans a wider range of the scattering angle than the more specular cases in Fig. 3, but still does not spread over all the hemisphere. The bi-directional reflection function of the other surface with $\sigma/\tau = 0.3$ shown in Fig. 4 is more angularly distributed. The energy is reflected diffusely through all the hemisphere, and no significant peaks occur.

The results of two very rough surfaces are illustrated in Fig. 5. The surfaces are described by $\sigma/\tau = 1.0$ and $\sigma/\tau = 3.0$. Since the rms deviation is on the order of the correlation length, the distribution is very diffuse and exhibits strong retro-reflection. For normal incidence, both exact and geometric optics results exhibit

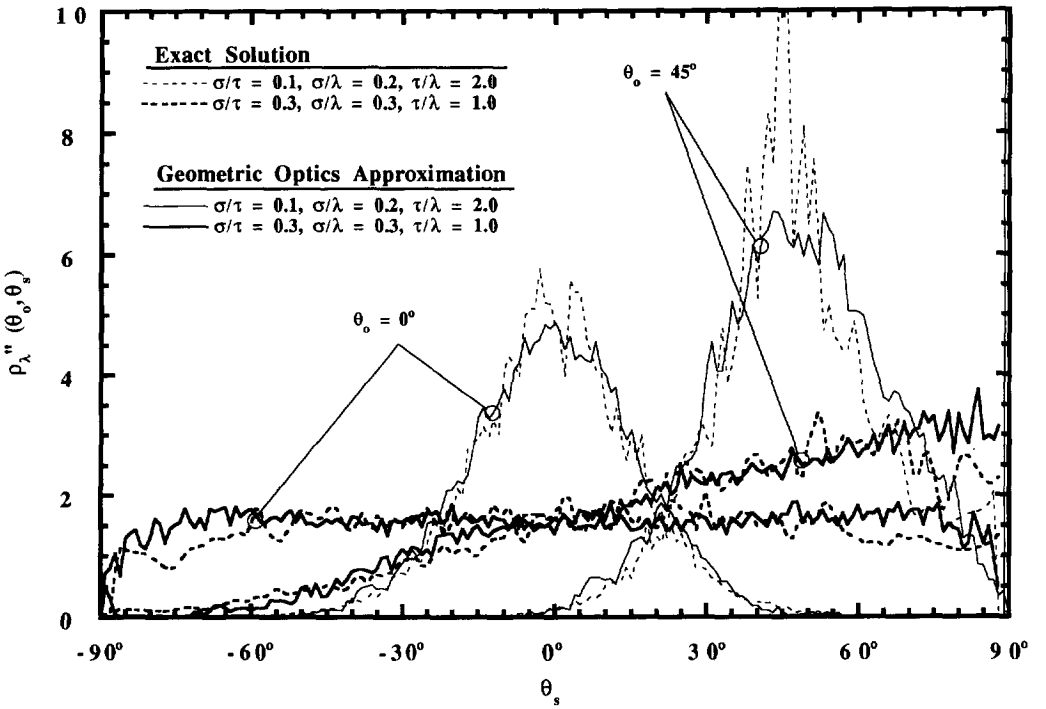

Fig. 4. Comparison of exact solutions with geometric optics approximations for the bi-directional reflection function at $\theta_o = 0°$ and 45° for rough surfaces.

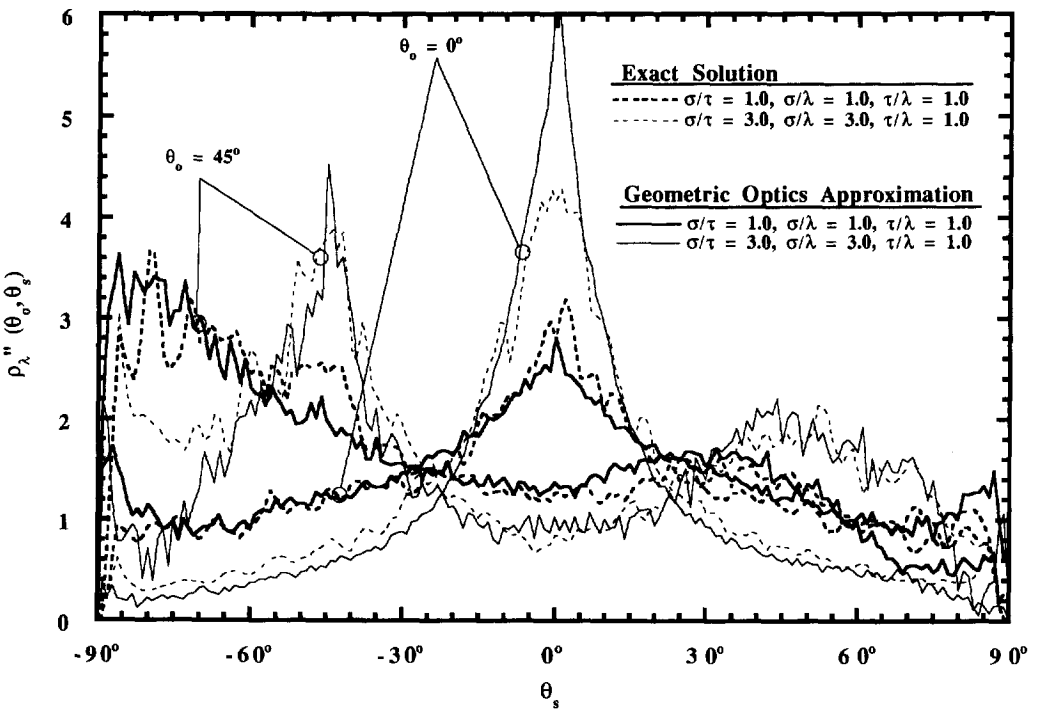

Fig. 5. Comparison of exact solutions with geometric optics approximations for the bi-directional reflection function at $\theta_o = 0°$ and 45° for very rough surfaces.

a single retro-reflection peak at normal scattering, $\theta_s = \theta_o = 0^\circ$. For the incident angle of $\theta_o = 45^\circ$, a slight enhancement in the angular region about $\theta_s = \theta_o = 45^\circ$ is observed, and a strong retro-reflection peak is observed at the anti-scattering angle of $\theta_s = -\theta_o = -45^\circ$.

Geometric optics and electromagnetic theory comparisons

Accurate approximations to electromagnetic scattering theory must faithfully characterize the directional distribution of scattered energy. Regardless of whether the phenomena is specular or diffuse, the approximation must correctly predict the scattering distribution. Therefore, a directional criterion that compares the angular nature of the exact solution and the approximation is needed.

In this work, the directional energy criterion, $\mathbf{E_d}$, used for comparing the angular nature of the exact solution and the geometric optics approximation is defined as the ratio of the difference in directional reflected energy predicted by the exact solution and by the approximation within an angular region $\Delta\theta_s$ to the averaged incident energy predicted by the exact solution. The ratio is evaluated over all directions in the hemisphere and the averaged difference is used in the criteria,

$$\mathbf{E_d} = \frac{\frac{1}{\pi}\sum_{n=1}^{\pi/\Delta\theta_s}\left|\int_{\Delta\theta_s} I_e\cos\theta_s\,d\theta_s - \int_{\Delta\theta_s} I_a\cos\theta_s\,d\theta_s\right|}{\frac{1}{\pi}\int_{-\pi/2}^{\pi/2} I_e\cos\theta_s\,d\theta_s} < \mathbf{E_{cr}} \tag{11}$$

where I is the intensity, θ_s is the scattering angle, and the subscripts e and a denote the exact solution and the geometric optics approximation, respectively. The averaged incident reflection is a constant for all incidence angles and surface parameters. If the ratio is less than a specific margin, $\mathbf{E_{cr}}$, then the two predictions are in good agreement and the approximation is considered valid.

The size of the angular region and the critical value could be determined for each individual application. $\Delta\theta_s$ could take values ranging from 180° for a comparison of hemispherical values to very small angles for directional comparisons. In the calculation presented here $\Delta\theta_s$ is selected to 1°. The criterion is useful for all surfaces, including non-perfectly conducting cases, although only perfectly conducting cases are considered here. The critical value for $\mathbf{E_{cr}}$ is taken as 0.20. The region of validity of the geometric optics approximate solution is quantified based on these rather restrictive values.

An alternate criterion focused in the angular region in the specular direction [10]. This criterion uses a finite angular region surrounding the specular angular region, $\Delta\theta_{SR}$, centered at $\theta_s = \theta_o$ [see Fig. 1(a) for definitions]. The criterion, $\mathbf{E_{SR}}$, is the ratio of the difference in the energy predicted by the approximate solution and by the exact solution relative to the energy predicted by the exact solution. Similarly, when this ratio is less than a specific margin then the two predictions are in good agreement and the approximation is considered valid. The criterion is expressed as follows:

$$\mathbf{E_{SR}} = \frac{\left|\int_{\Delta\theta_{SR}} I_e\cos\theta_s - I_a\cos\theta_s\,d\theta_s\right|}{\int_{\Delta\theta_{SR}} I_e\cos\theta_s\,d\theta_s} < \mathbf{E_{cr}}. \tag{12}$$

The angular region, $\Delta\theta_{SR}$, is set to 20° ($\theta_o \pm 10^\circ$). I_a is the intensity predicted by the geometric optics approximation, while I_a in ref. [10] is a simple Fresnel Dirac delta function. Note that $\mathbf{E_d}$ requires accuracy for $\Delta\theta_s = 1^\circ$ over the entire domain of θ_s while $\mathbf{E_{SR}}$ considers a relatively large region of about the specular angle only.

The exact solutions for the relatively smooth surface presented in Fig. 3 are not well approximated by the geometric optics solution except the case of normal incidence on the surface with $\sigma/\tau = 0.02$ in which $\mathbf{E_d} = 0.198$. The failure occurs because the energy difference [numerator of equation (11)] is on the order of or larger than the averaged incident energy [denominator of the equation (11)]. In Fig. 4, the exact solution of the surface described by $\sigma/\tau = 0.1$ is fairly well approximated by the geometric optics solution at the normal incidence. The ratio, $\mathbf{E_d}$, is 0.129. As the incidence angle increases to 45°, $\mathbf{E_d}$ increases to 0.231 which is larger than the chosen critical value, $\mathbf{E_{cr}} = 0.20$; thus, the approximation is considered invalid. For the diffuse reflection surface described by $\sigma/\tau = 0.3$ shown in Fig. 4, the exact and geometric optics results are in good agreement. The values of $\mathbf{E_d}$ are 0.085 and 0.089 for $\theta_o = 0^\circ$ and 45°, respectively. For all the cases of very rough surfaces presented in Fig. 5, the geometric optics approximation is valid. The values of $\mathbf{E_d}$ are 0.082 and 0.108 for the surface with $\sigma/\tau = 1.0$ at $\theta_o = 0^\circ$ and 45°, and 0.151 and 0.164 for the surface with $\sigma/\tau = 3.0$. The values of $\mathbf{E_d}$ not only imply that incident angles have a strong influence on the accuracy of the approximation but also the ratio σ/τ.

Figure 6 shows the parameter domain of validity for the geometric optics approximation for a critical value, $\mathbf{E_{cr}} = 0.2$. The entire region below each solid line on the graph is the region of validity for the geometric optics approximation. Both the exact solution and the geometric optics approximation conserve energy within 1%. Approximately 40 different surfaces were compared to make Fig. 6 with the correlation lengths ranging from $\tau/\lambda = 0.1$ to $\tau/\lambda = 10.0$. The range of rms deviation is from $\sigma/\lambda = 0.01$ to $\sigma/\lambda = 10.0$, corresponding to a range of the ratio σ/τ

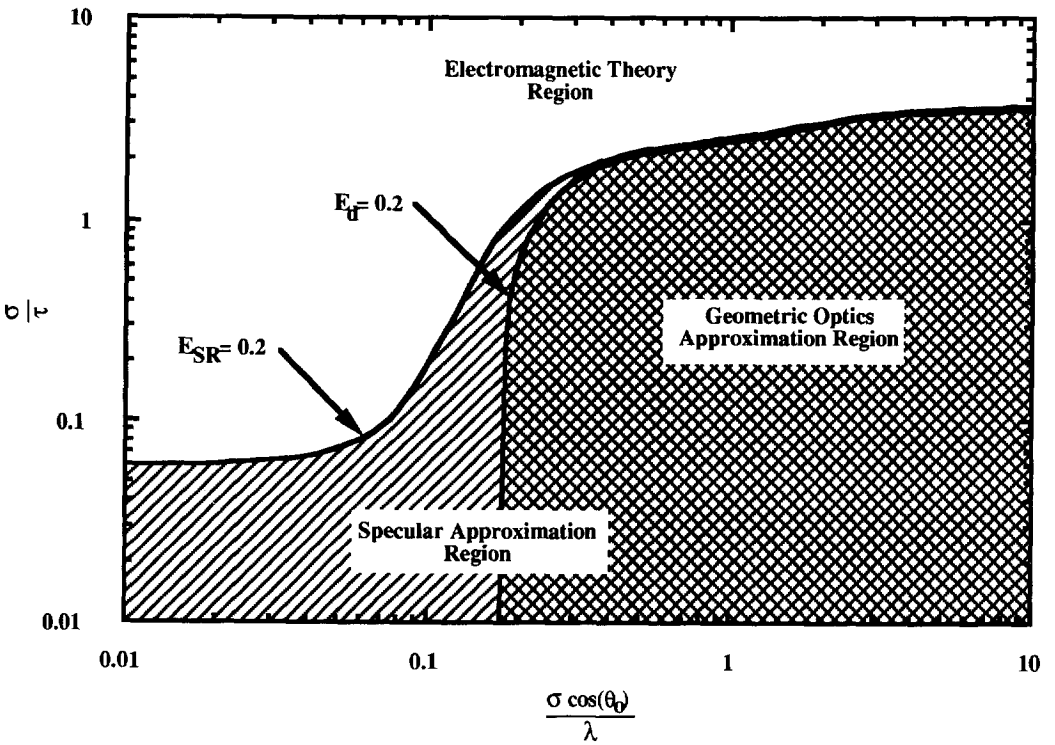

Fig. 6. Electromagnetic theory rough surface scattering domain plot with regions validity for the geometric optics and specular approximations, $\Delta\theta_s = 1^\circ$ and $\Delta\theta_{SR} = 20^\circ$.

from 0.01 to 4.0. A majority of the calculations were performed in the regions near of the solid lines. Over 60 surface realizations were used for both the exact predictions and the geometric optics approximation. Due to the very rough nature of many of the surfaces compared in Fig. 6, the exact solution is inaccurate at incident angles larger than 45° and conservation of energy for the surface fails. Therefore, the results at incident angles larger than 45° are not reported.

It is commonly believed the geometric optics approximation can only be applied for a surface which has τ/λ and $\sigma/\lambda \gg 1$. As shown in Fig. 6, the geometric optics approximation works well even when τ/λ and σ/λ are less than unity. However, as $(\sigma/\lambda)\cos\theta_0$ diminishes, the validity of the geometric optics approximation requires a small ratio σ/τ, and no geometric optics solution can approximate the exact solution for surfaces which have a $(\sigma/\lambda)\cos\theta_0$ less than 0.17 for the domain considered in Fig. 6 (i.e. for $\sigma/\tau \geqslant 0.01$). The strong influence of the ratio σ/τ on the validity of the geometric optics approximation is clearly illustrated in Fig. 6. For instance, at $\theta_0 = 30^\circ$ and for $\sigma/\lambda = 0.3$, the $\mathbf{E}_d$ increases from 0.09 to 0.12 as the σ/τ increases from 0.33 to 0.60. In fact, the geometric optics approximation boundary becomes horizontal as the slope approaches $\sigma/\tau = 4.0$. Thus, surfaces with a slope greater than 4.0 are not well approximated by the geometric optics solution.

Several dielectric cases have been studied and compared to the perfectly conducting surfaces. Cases within the domain and near the boundary have been considered. Due to the very rough nature of many surfaces, the exact solution of dielectric cases is inaccurate at incident angles larger than 45°. Also, due to computational limitations, the exact solutions for $\sigma/\tau > 1.0$ would require more than 300 Megawords of memory and 30 h of CPU time and they have not been calculated.

The domain of perfectly conducting surfaces for the geometric optics approximation for the critical value, $\mathbf{E}_{cr} = 0.20$ should be a conservative estimate for dielectric materials. For smooth surfaces, the values of $\mathbf{E}_d$ for both dielectric and for perfectly conducting cases are very similar. For rough surfaces, the geometric optics approximation is slightly more accurate for dielectric cases than perfectly conducting cases. In general, the values of $\mathbf{E}_d$ for dielectric surfaces are lower than for perfectly conducting surfaces for rough and very rough cases. The geometric optics approximation should be more accurate for dielectric cases since, for a perfectly conducting rough surface, the second and third scatterings dominate the solution. For dielectric materials, only a fraction of the incident energy is reflected after each scattering (the rest of the energy is transmitted through the surface interface), and the energy in the double and triple scatterings is smaller than single scattering. The surface reflection is then dominated by single scattering. Even though no dielectric cases with $\sigma/\tau > 1.00$ could be compared to the exact solution, it seems likely that geometric optics approximation will continue to be valid beyond $\sigma/\tau > 1.00$ within the domain shown in Fig. 6.

If a surface is well approximated by the geometric optics approximation, then the computational cost to obtain the exact solution is not justified. The exact solution for dielectric surfaces takes approximately 100 Megawords of memory and 14 h of CPU time to predict the averaged scattering from 60 very rough surface realizations. The geometric optics approximation takes approximately one hundredth of the memory and one tenth of the CPU time to predict the scattering. If an exact reflection distribution or specific magnitude of reflected energy at a certain θ_s is desired, then the exact solution must be used.

Based on the specular criterion in equation (12), the exact solution for the smooth surfaces illustrated in Fig. 3 is well approximated by the geometric optics solution for incident angles of 0° and 45° since 99% of the reflected energy, $\mathbf{E_{SR}} = 0.01 < \mathbf{E_{cr}}$, is contained within the region described by $\Delta\theta_{SR} = 20°$. Also by this criterion, the geometric optics approximation is valid for all the cases presented in Figs. 4 and 5. In Fig. 6, the entire region for which the geometric optics approximation is valid based on the directional criterion (the area denoted by ▨) is covered by the region justified by the specular criterion (the area denoted by ▨). The directional criterion suggests that the geometric optics solution should not apply on any surface which has a $(\sigma/\lambda)\cos\theta_o$ less than approximately 0.17 for σ/τ greater than 0.01. However, based on the less restrictive specular criterion, the region for which the geometric optics approximation can be applied can be extended beyond $(\sigma/\lambda)\cos\theta_o = 0.17$. In fact, the specular criterion suggests the geometric optics approximation can be applied for the region in the domain where $(\sigma/\lambda)\cos\theta_o$ is as low as one hundredth, given that σ/τ is smaller than 0.06. On the other hand, when the ratio σ/τ is larger than 0.5, two regions approach each other. It means that $\mathbf{E_d} \approx \mathbf{E_{SR}}$ in the region just below the line. Clearly, the directional criterion is more restrictive than the specular criterion.

CONCLUSIONS

The geometric optics approximation of electromagnetic scattering theory can be used to accurately characterize the scattering from many random rough surfaces. Unlike the Dirac delta function of the Fresnel approximation, the geometric optics approximation is a multiple scattering solution. Therefore, it has the ability to predict both specular and diffuse reflection. In the limit of a plane surface, the geometric optics approximation reduces to the simple Fresnel approximation. Unlike this specular approximation which predicts the scattered energy in the specular spike for every incident angle, the geometric optics approximation changes from diffuse scattering to retro-reflection with the incident angle. The geometric optics approximation can accurately predict retro-reflection.

The incident angle, the ratio of rms deviation to correlation length, and the ratio rms deviation to the wavelength are shown to have a strong influence on the accuracy of the geometric optics approximation. A directional criterion is established to evaluate the accuracy of the geometric optics approximation. The criterion which based on very small angular regions of one degree including all angles

The parameter domain of validity for the geometric optics approximation on perfectly conducting surfaces is given in Fig. 6. Several dielectric cases within the domain and near the boundary of the domain have been studied and compared to perfectly conducting cases. The geometric optics approximation appears to be also valid within the domain.

Using the geometric optics approximation represents a significant reduction in computational time and memory, since the matrices in the electromagnetic scattering integrals are not solved. The geometric optics approximation represents a reduction of approximately one hundredth in memory and takes one fifth the time. When a reflection distribution is needed and the approximation provides an accurate result, the geometric optics method provides a computationally inexpensive solution which accurately predicts the angular scattering phenomena from random rough surfaces.

Acknowledgements—This research was supported, in part, by the Richard W. Kritzer Endowment Fund, Pittsburgh Supercomputing Center, Pittsburgh, Pennsylvania, and the National Center for Supercomputing Applications, Urbana, IL, U.S.A.

REFERENCES

1. K. G. T. Hollands, Directional selectivity, emittance, and absorptance, properties of Vee corrugated specular surfaces, *Solar Energy* **7**, 108–116 (1963).
2. P. Demont, M. Huetz-Aubert and H. Tran N'Guyen, Experimental and theoretical studies of the influence of surface conditions on radiative properties of opaque materials, *Int. J. Thermophys.* **3**, 335–364 (1982).
3. P. J. Hesketh, J. N. Zemel and B. Gebhart, Measurements of the spectral and directional emission from microgrooved silicon surfaces, *J. Heat Transfer* **110**, 680–686 (1988).
4. E. Wolf, A generalized extinction theorem and its role in scattering theory. In *Coherence and Quantum Optics* (Edited by E. Wolf), pp. 339–357. Plenum, New York (1973).
5. V. Celli, A. A. Maradudin, A. M. Marvin and A. R. McGurn, Some aspects of light scattering from a randomly rough metal surface, *J. Opt. Soc. Am. A* **2**, 2225–2239 (1985).
6. A. A. Maradudin, T. Michel, A. R. McGurn and E. R. Méndez, Enhanced backscattering of light from a random grating, *Ann. Phys.* **203**, 255–307 (1990).
7. A. A. Maradudin, E. R. Méndez and T. Michel, Backscattering effects in the elastic scattering of p-polarized light from a large-amplitude random metallic grating, *Opt. Lett.* **14**, 151–153 (1989).
8. J. A.Sánchez-Gil and M. Nieto-Vesperinas, Light scattering from random dielectric surfaces, *J. Opt. Soc. Am. A* **8**, 1270–1286 (1991).
9. M. Nieto-Vesperinas and J. A. Sánchez-Gil, Light scat-

tering from a random rough interface with total internal reflection, *J. Opt. Soc. Am. A* **9,** 424–436 (1992).
10. R. A. Dimenna and R. O. Buckius, Quantifying specular approximations for angular scattering from perfectly conducting random rough surfaces, *J. Thermophys. Heat Transfer* **8,** 393–399 (1994).
11. E. I. Thorsos, The validity of the Kirchhoff approximation for rough surface scattering using a Gaussian roughness spectrum, *J. Acoust. Soc. Am.* **83,** 78–92 (1988).
12. J. M. Soto-Crespo and M. Nieto-Vesperinas, Electromagnetic scattering from very rough random surfaces and deep reflection gratings, *J. Opt. Soc. Am. A* **6,** 367–384 (1989).
13. M. F. Chen and A. K. Fung, A numerical study of the regions of validity of the Kirchhoff and small-perturbation rough surface scattering models, *Rad. Sci* **23,** 163–170 (1988).
14. D. H. Berman and J. S. Perkins, The Kirchhoff approximation and first-order perturbation theory for rough surface scattering, *J. Acoust. Soc. Am.* **78,** 1045–1051 (1985).
15. J. A. Stratton, *Electromagnetic Theory*, pp. 23–131. McGraw-Hill, New York (1941).
16. M. Q. Brewster, *Thermal Radiative Transfer and Properties* (1st Edn), pp. 28–156. John Wiley, New York (1992).
17. A. K. Fung and M. F. Chen, Numerical simulation of scattering from simple and composite random surfaces, *J. Opt. Soc. Am. A* **2,** 2274–2284 (1985).
18. R. A. Dimenna and R. O. Buckius, Electromagnetic theory predictions of the directional scattering from triangular surfaces, *J. Heat Transfer* **116,** 639–645 (1994).
19. P. M. Morse and H. Feshbach, *Methods of Theoretical Physics* 1 *and* 2, p. 155. Technology Press, Cambridge, MA (1946).
20. Y. Yang and R. O. Buckius, Surface length scale contributions to the directional and hemispherical emissivity and reflectivity, *J. Thermophys. Heat Transfer* **9,** 653–659 (1995).